

Opposing effects of dietary sugar and saturated fat on cardiovascular risk factors and glucose metabolism in mitochondrially impaired mice

Doreen Kuhlow · Kim Zarse · Anja Voigt ·
Tim J. Schulz · Klaus J. Petzke · Lutz Schomburg ·
Andreas F. H. Pfeiffer · Michael Ristow

Received: 7 September 2009 / Accepted: 22 February 2010 / Published online: 10 March 2010
© Springer-Verlag 2010

Abstract

Purpose Both dietary fat and dietary sucrose are major components of Western diets that may differentially affect the risk for body mass gain, diabetes mellitus, and cardiovascular disease.

The authors Doreen Kuhlow, Kim Zarse, Anja Voigt contributed equally to this work.

Electronic supplementary material The online version of this article (doi:10.1007/s00394-010-0100-4) contains supplementary material, which is available to authorized users.

D. Kuhlow · K. Zarse · T. J. Schulz · M. Ristow (✉)
Department of Human Nutrition, Institute of Nutrition,
University of Jena, 07743 Jena, Germany
e-mail: mristow@mristow.org

D. Kuhlow · A. Voigt · T. J. Schulz ·
A. F. H. Pfeiffer · M. Ristow
Department of Clinical Nutrition, German Institute of Human
Nutrition Potsdam-Rehbrücke, 14558 Nuthetal, Germany

K. J. Petzke
Stable Isotope Group, German Institute of Human Nutrition
Potsdam-Rehbrücke, 14558 Nuthetal, Germany

L. Schomburg
Institute of Experimental Endocrinology,
Charité University Medicine, 13353 CVK, Berlin, Germany

A. F. H. Pfeiffer
Department of Endocrinology, Diabetes and Nutrition,
Charité University Medicine, 12203 CBF, Berlin, Germany

Present Address:

T. J. Schulz
Research Section Obesity and Hormone Research,
Joslin Diabetes Center, Harvard Medical School,
Boston, MA 02215, USA

Methods We have phenotypically analyzed mice with ubiquitously impaired expression of mitochondrial frataxin protein that were challenged with diets differing in macronutrient content, namely high-sucrose/low-fat and high-saturated fat/low-sugar diets.

Results We find here that a high-sucrose/low-fat diet has especially detrimental effects in mice with impaired mitochondrial metabolism promoting several independent cardiovascular risk factors, including impaired glucose metabolism, fasting hyperinsulinemia, reduced glucose-stimulated insulin secretion, increased serum triglycerides, and elevated cholesterol levels due to increased expression of HMG-CoA reductase. In contrast, a high-saturated fat/low-sugar diet protects mice with impaired mitochondrial metabolism from diet-induced obesity by increasing total energy expenditure and increasing expression of ACAA2, a rate-limiting enzyme of mitochondrial beta-oxidation, whereas no concomitant improvement of glucose metabolism was observed.

Conclusions Taken together, our results suggest that mitochondrial dysfunction may cause sucrose to become a multifunctional cardiovascular risk factor, whereas low-sugar diets high in saturated fat may prevent weight gain without improving glucose metabolism.

Keywords Mitochondria · Macronutrient metabolism · Diabetes · Obesity · Cardiovascular disease

Introduction

In Western countries, both dietary sugars as well as saturated fatty acids represent increasingly important components of human diets [2, 3, 5, 6, 8, 10, 17, 18, 23, 31, 35]. Specifically, in US-Americans, sugars account for 25% of

daily calorie intake [11] and have been shown to negatively affect serum lipoprotein profiles promoting dyslipidemia in humans [20]. Accordingly, it has been recommended to reduce intake of nutritive sucrose in order to minimize cardiovascular disease risk [11, 16, 36]. Nevertheless, it has been repeatedly observed that individual response to dietary measures differs tremendously between subjects [33], suggesting an unknown systemic mechanism determining the fate of ingested sugars with regards to undesirable effects on risk for cardiovascular disease. Risk factors include four key features of the so-called metabolic syndrome, namely hyperglycemia, fasting hyperinsulinemia, hypertriglyceridemia, and hypercholesterolemia [25].

Regarding the underlying biochemical cause, we hypothesized that reduced efficiency of mitochondrial metabolism might prevent the key intermediate of cellular sucrose breakdown, acetyl-CoA, from being oxidized to carbon dioxide, thereby inducing *de novo* synthesis of lipids, including cholesterol, from acetyl-CoA. Unlike generation of carbon dioxide and of the concomitant proton gradient, this process requires only minimal mitochondrial activity. To test this hypothesis, we have used mice with ubiquitously reduced expression of the mitochondrial protein frataxin, which exhibit a limited impairment of mitochondrial capacity in a non-tissue-specific manner, as previously described [22]. As shown there, these frataxin knock-down mice develop obesity only when maintained on a so-called Western diet containing excessive amounts of both sucrose and saturated fat; while a less energy-dense, polysaccharide-rich rodent diet fully prevents this phenotype [22]. We now show that maintaining these knock-down animals on a sucrose-enriched/low-fat diet promotes several independent cardiovascular risk factors, including impaired glucose metabolism, fasting hyperinsulinemia, reduced glucose-stimulated insulin secretion, increased serum triglycerides, and elevated cholesterol levels, suggesting that impaired mitochondrial metabolism may convert sucrose into a significant health threat. In contrast, replacing sucrose by dietary fat in an isocaloric manner prevents the afore-mentioned alterations and rather protects from weight gain in this model of impaired mitochondrial metabolism.

Materials and methods

Generation of mice

For generation of mice with mitochondrial dysfunction, expression of the mitochondrial protein frataxin was downregulated by employing the Cre-loxP-recombinase-system. Namely, frataxin expression was impaired by loxP-

Table 1 Composition of diets

	'High-sugar'	'High-fat'
Proteins (casein, g/kg)	95	92
Polysaccharides (corn starch, g/kg)	362	338
Disaccharides (sucrose, g/kg)	364	13
Lipids (palm fat, g/kg)	51	231
Cholesterol (g/kg)	<0.001	<0.001
Convertible energy (kJ/g)	16	16

targeting exon 4 of the corresponding gene as described [22, 24, 26], except that systemic expression of Cre recombinase was obtained by using a subline of mice carrying an aP2-promotor-driven Cre transgene [1, 22]. Expression of aP2-driven Cre recombinase was obtained with a single founder kindly provided by BIDMC (Boston, MA, USA) reported to be 90% C57BL/6. Frataxin knock-down mice were derived by intercrossing frataxin loxP heterozygous mice (frataxin^(+/lox)) with frataxin loxP heterozygous mice that also expressed Cre recombinase under the control of the aP2 promotor/enhancer (frataxin^(+/lox) aP2Cre^(+/-)). Consequently, frataxin knock-down mice have the genotype Cre^(+/-) frataxin^(lox/lox). The remaining genotypes, frataxin^(+/+), frataxin^(+/lox), frataxin^(lox/lox) (all without Cre), and frataxin^(+/+) Cre^(+/-), were used as controls. At an age of 30 weeks, frataxin knock-down and wild-type controls were matched for gender and body mass and placed on the three experimental diets. Mice at this age were chosen to avoid developmental effects of different diets. For most experiments, cre-positive and loxP-negative animals were additionally studied and showed no significant differences versus wild-type control animals. Low-caloric, low-fat, fiber-rich standard rodent chow (Altromin 1324) (convertible energy, 9 kJ/g; lipids, 40 g/kg; polysaccharides, 317 g/kg) [22]; high-caloric, high-sucrose-diet (Table 1) and high-caloric, high-fat diet (Table 1) were custom-made and obtained from Altromin GmbH, Lage, Germany. Animals were housed in air-conditioned rooms (temperature, 20 ± 2 °C; relative moisture, 50–60%) under a 12-h-light/dark schedule (lights on at 06:00 h) and had free access to chow and water. They were kept in accordance with the National Institutes of Health guidelines for the care and use of laboratory animals, and all experiments were approved by the ethics committee of the Ministry of Agriculture, Nutrition, and Forestry (State of Brandenburg, Germany).

Genotype determinations

Genomic PCRs for detection of the loxP allele and the Cre transgene were performed as described [22, 26].

ATP content determinations

Liver tissue for ATP-determination was removed in the fed state, namely 2 h after beginning of the active dark phase at 20:00 h, and immediately clamp-frozen. Methods for ATP-measurements have been described [7, 22].

Body composition analysis

Body weight and body composition (including fat content) were measured as previously described, including use of quantitative nuclear magnetic resonance technique (Bruker Minispec mq10, Bruker Optics Inc., Billerica, MA) [22].

Food consumption quantification

Food intake was measured three times per week by weighing (BP 2100, Sartorius AG, Göttingen, Germany; detection limit 0.01 g) and normalized to 24 h and g of total body mass as previously described [22].

Respiratory quotient and total energy expenditure

Total energy expenditure and respiratory quotient were determined by indirect calorimetry of mice housed individually in metabolic cages, receiving food and water ad libitum as described [13]. Gas analysis was performed using the analyzing system Advanced Optima (ABB, Mannheim, Germany; former Hartmann & Braun GmbH & Co. KG, Frankfurt/Main, Germany) containing oxygen (Magnos 16) and a carbon dioxide (Uras 14) analyzer. Calorimetric measurements were performed for 48 h in parallel and every six min after an acclimation period of 24 h. Total energy expenditure was normalized to 24 h and metabolic body mass [13].

Glucose tolerance tests

Glucose tolerance tests were performed as described [26] by intraperitoneal (IP) glucose injection (D-(+)-glucose, Merck, Darmstadt, Germany) after mice were fasted 16 h overnight. Serum was collected before and 10, 30, and 120 min after glucose challenge and immediately frozen at -80°C for measurement of glucose and insulin. If not indicated otherwise, GTTs were performed 6 weeks after initiation of diets.

Serum analyses

Blood samples for glucose measurements were obtained both in the fed state as well as after mice were fasted 16 h overnight. Determination of serum lipid concentrations was performed in samples collected after a 16-h overnight

fasting period. Blood was collected by retro-orbital puncture. Serum samples were immediately prepared by centrifugation, and immediately frozen at -80°C for further measurements as described [26].

Determination of glucose, non-esterified fatty acids (NEFA), triglycerides, and total cholesterol in serum was performed by using automated analyzer (Cobas Mira S, Hoffmann-La Roche, Basel, Switzerland) employing commercial kits (glucose HK125, triglycerides and total cholesterol from ABX, Montpellier, France, and NEFA C from Wako, Neuss, Germany). Mouse serum insulin levels were measured by ELISA for rat insulin using a mouse insulin standard (both from Crystal Chem Inc., Chicago, Illinois, USA) as described [26].

Immunoblots

Western blotting was performed on protein extracts obtained from clamp-frozen liver tissues collected in the fed state at 20:00 h. Liver tissue samples of four animals per diet and genotype were clamp-frozen, and protein was extracted by using Sörenson's phosphate buffer. After analyzing the protein content by using the Bradford assay, the protein extract was heated for 5 min at 95°C with Laemmli buffer and DTT and finally stored at -20°C until immunodetection. After SDS-PAGE, immunodetection was performed using primary antibodies against HMG-CoA-reductase (Anti-HMG-CoA Reductase, #07-457, Upstate, Lake Placid, NY, USA) and Acetyl-CoA-Acyl-transferase 2 (ACAA2) (Anti-ACAA2, Clone 5C4, #H00010449-M01, Abnova Corporation, Taipei City, Taiwan) as well as alpha-Tubulin (Anti-alpha-Tubulin, Clone DM 1A, #T9026, Sigma, Taufkirchen, Germany) were used. Specific signals were detected (ECL Detection Reagents, Amersham Biosciences, Freiburg, Germany), quantified with luminescence imaging (LAS-1000, Fuji-film, Japan) and quantification software (AIDA, Raytest, Germany), and normalized to α -tubulin signals.

$^{13}\text{C}_2$ breath tests for glucose oxidation experiments

$^{13}\text{C}_2$ breath tests were applied as non-invasive methods to study the oxidation of injected or ingested ^{13}C -labeled glucose. The tests were performed in parallel between 0800 and 1700, in eight male mice of each genotype with free access to food and water. The ^{13}C -labeled substrate used in this study was D-glucose (U- $^{13}\text{C}_6$, 98%, M = 181.6 g/mol; Cambridge Isotope Lab., Inc., Woburn, MA, USA). Ten micromoles per kg ^{13}C -labeled glucose dissolved in sterilized 0.154 mol/l NaCl, and a volume of 50 μL /20 g body weight was injected intraperitoneally. Breath samples for determination of ^{13}C -glucose oxidation were obtained at baseline and at 10, 20, 30, 40, 50, 60, 80, 100, and

120 min in duplicate after injection, respectively. In order to collect $^{13}\text{CO}_2$ samples, mice were placed individually at each time point for 30 s into 140-mL syringes. This time interval was tested to be sufficient in CO_2 concentration and ^{13}C enrichment for mice (data not shown). The syringes were equipped with a wave to collect representative breath samples into evacuated 10-mL tubes (Exetainer, Labco Ltd., High Wycombe, U.K.) for storage and measurement.

Breath $^{13}\text{CO}_2$ enrichments were analyzed by isotope ratio mass spectrometry (BreathMAT, Thermo Scientific Corp., Bremen, Germany) and were expressed as $\delta^{13}\text{C}$ in the conventional delta per mill notation as described [21]. The delta over baseline values (DOB) were calculated by taking the difference between enrichments of each breath sample and the baseline breath sample. The baseline ^{13}C abundances in breath CO_2 (data not shown) were in accordance to a consumption of C_3 plant-based experimental diets with a relatively low natural ^{13}C abundance before the breath tests.

RNA extraction and RNA array analyses

RNA was extracted from tissue samples according to the TRIzol method (Invitrogen) according to the manufacturer's instructions. Crude RNA was subsequently loaded onto an RNA binding column (QIAGEN) to remove contaminating genomic DNA and proteins before further processing. Total RNA content was assayed, and equal amounts of RNA were used for cDNA synthesis and hybridization. For transcript-level analysis, the Affymetrix Mouse Genome 430 2.0 Array was used according to the manufacturer's instructions. Analysis of the presented data was performed with Affymetrix GCOS software by comparing means of signal intensities from RNA samples derived from control and knock-down animals. Ratios for transcript-level regulation as control versus knock-down signal intensities were obtained to illustrate the extent of regulation (Affymetrix GCOS software; threshold for regulation was set to 1.50). As individual transcripts are represented by a set of different probes on the chip, transcripts were only considered to be regulated when at least two-thirds of probes for the same transcript displayed similar regulation. Genes which were expressed at a fold change ratio greater than 1.5 in knock-down animals compared to controls were subjected to metabolic pathway analysis using the Gene Set Enrichment Analysis (GSEA) Software [19, 30].

Data analysis

Data are expressed as mean \pm SEM. Equal distributions were tested by Kolmogorov–Smirnov test before applying

T-tests. Unpaired Student's *T*-tests were used to compare knock-down and wild-type control animals of each dietary group as well as a two way ANOVA (diet, genotype) for analyzing the glucose clearance in the glucose tolerance test both by employing SPSS 15.0 (SPSS, Chicago, IL, USA).

Results and discussion

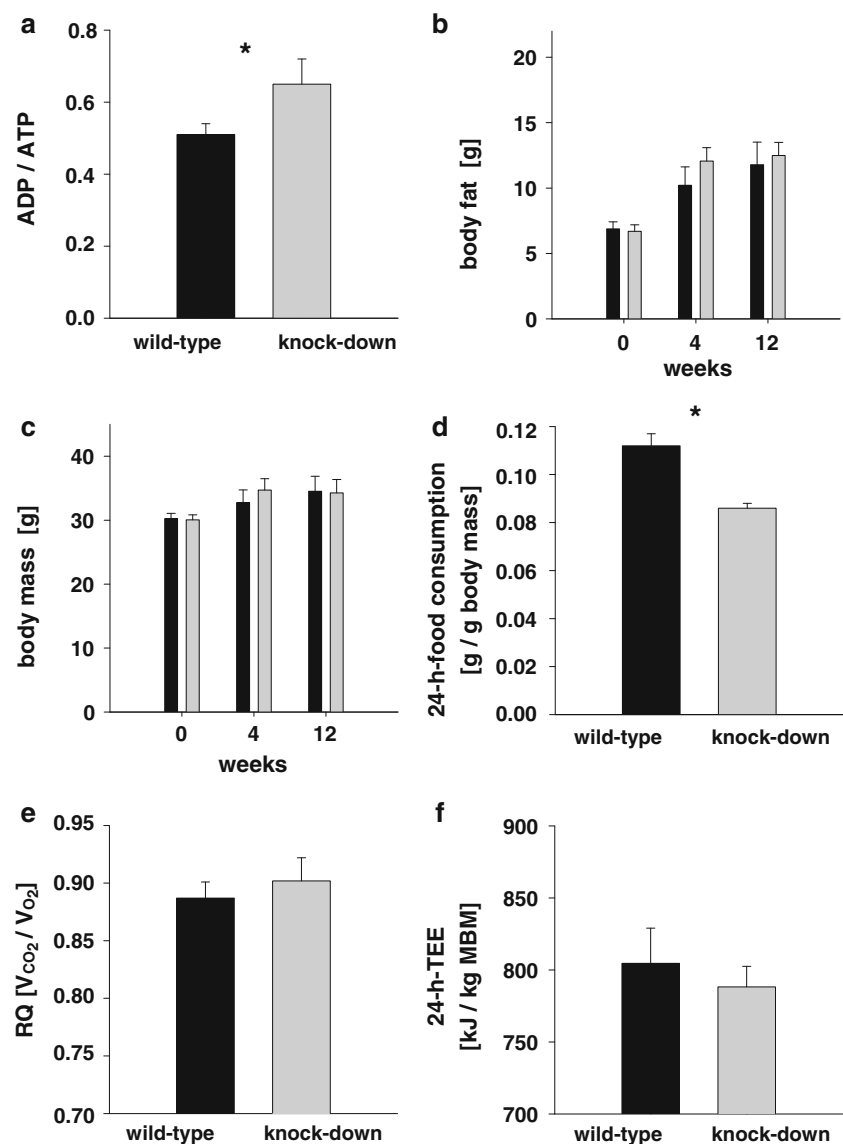
A high-sucrose diet reduces food uptake in mitochondrially impaired mice

Our previous study has shown that impaired frataxin expression in mice in an ubiquitous manner causes impaired mitochondrial metabolism and promotes weight gain following Western diet exposure due to impaired energy expenditure [22].

To further dissect the role of different macronutrients and specifically dietary sucrose in mammals, we have studied frataxin knock-down mice and their wild-type littermates at an age of 30 weeks. At this age, and comparable to young knock-down animals [22], they still show impaired mitochondrial function, as shown by an increased ratio of adenosine-diphosphate (ADP) to adenosine-triphosphate (ATP) in liver specimen obtained from these animals (Fig. 1a).

We have placed such mice and corresponding littermates on a diet containing high amounts of sucrose (Table 1) at an age of 30 weeks; the study was terminated at an age of 43 weeks. Unlike Western diets used for previous experiments [22], the high-sucrose diet used in this study did not contain cholesterol and was comparably low in total fat content, whereas convertible energy content was similar to that of previous experiments employing a Western diet [Table 1; 22]. When maintained on this particular diet, mitochondrially impaired knock-down mice showed body fat content (Fig. 1b) as well as body mass (Fig. 1c) similar to that of wild-type controls. We observed reduced daily food intake in knock-down mice (Fig. 1d, $P = 0.008$), whereas respiratory quotient (Fig. 1e) and total energy expenditure (TEE) (Fig. 1f) did not differ significantly between the two study groups. Therefore, it should be noted that all phenotypical alterations described below for these mice on a high-sugar diet are not related to obesity (Figs. 1b, c) and rather occur despite a significantly decreased energy intake (Fig. 1d) while food absorption has not been quantified. Furthermore, it should be noted that these animals, when being maintained on a Western diet, significantly gained body fat [22] whereas this seems not to be the case on the high-sucrose diet used in the present study (Table 1, Fig. 1b, c).

Fig. 1 Reduced mitochondrial metabolism does not affect body mass on a high-sucrose diet. **a** Ratio of hepatic ADP and ATP content in high-sucrose-fed mice; *black bars* correspond to control animals (“wild-type”), while *gray bars* reflect frataxin knock-down animals with impaired mitochondrial capacity (applies to all subsequent panels except for 3E and 4G) ($n = 5$ per genotype). *Error bars* reflect standard error of means, star indicates $P < 0.05$ (applies to all subsequent panels). **b** Body fat content in mice as in *Panel A* ($n = 10$ per genotype). **c** Body mass of mice as in *Panel A* ($n = 10$ per genotype). **d** Food uptake per individual mouse, depicted for mice as in *Panel A* ($n = 6$ per genotype). **e** Individual respiratory quotient of mice as in *Panel A* ($n = 6$ per genotype). **f** Total energy expenditure of mice as in *Panel A* ($n = 6$ per genotype)



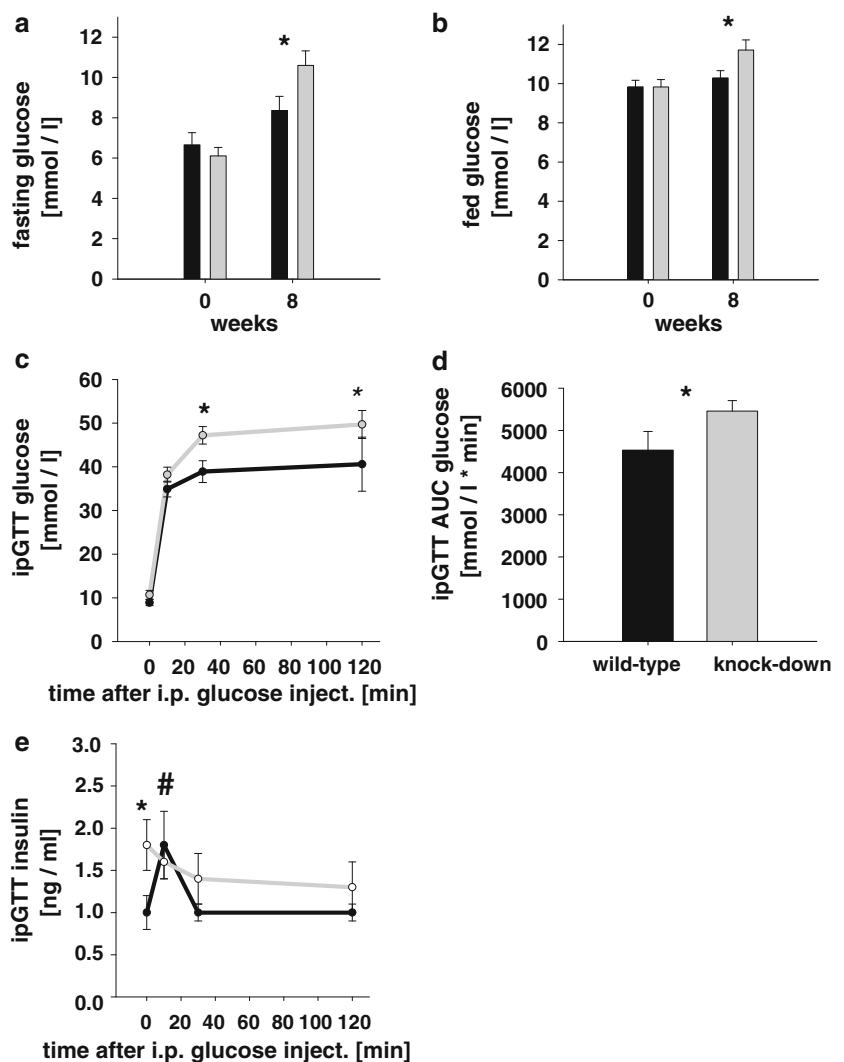
Impaired glucose metabolism and reduced glucose-induced insulin secretion in sucrose-fed mitochondrially impaired mice

Next, we quantified glucose metabolism as previously described [26] and observed increased fasting serum glucose levels exclusively in mitochondrially impaired mice on a high-sucrose diet (Fig. 2a, $P = 0.047$). Accordingly, postprandial serum glucose levels were found to be elevated only in mitochondrially impaired mice on a high-sucrose diet (Fig. 2b, $P = 0.035$). While no differences in body mass were observed, as previously stated (Fig. 1c), intraperitoneal injection of D-glucose as described before [26] revealed a significant impairment of glucose disposal rates in mitochondrially impaired mice on a high-sucrose diet (Fig. 2c, $P = 0.024$), whereas no differences were observed in mice on standard rodent chow (data not

shown). Similar differences were observed for the areas under the curves (AUCs) for glucose excursion after intraperitoneal injection of glucose (Fig. 2d, $P = 0.049$).

Quantification of serum insulin concentrations revealed increased levels during the fasting state only in mitochondrially impaired mice on high-sucrose diet (Fig. 2e, 0 min, $P = 0.024$ wild-type vs. knock-down genotype), while no differences were observed in mice on standard rodent diet (data not shown). This fasting hyperinsulinemia was accompanied by a complete loss of the so-called first-phase insulin secretion, which typically occurs a few minutes after injection of D-glucose in genetically unaltered animals. While control littermates still exhibited first-phase secretion on a high-sucrose diet (Fig. 2e, increases from 0 to 10 min after injection: $P = 0.034$ for wild-type, $P = 0.571$ for knock-down genotype), no differences were observed in mice on standard rodent diet (data not shown).

Fig. 2 Reduced mitochondrial metabolism causes impaired glucose metabolism in mice on a high-sucrose diet independent of body mass. **a** Fasting serum glucose levels of mice that were food deprived for 16 h ($n = 8$ per genotype). **b** Postprandial serum glucose levels of mice that had free access to sucrose-enriched diet ($n = 8$ per genotype). **c** Serum glucose excursions following intraperitoneal injection of D-glucose; *black line* corresponds to control animals, while *gray line* reflects frataxin knock-down animals with impaired mitochondrial capacity (also applies to panel E) ($n = 8$ per genotype); **d** Area under the curves (AUCs) for glucose excursions ($n = 8$ per genotype). **e** Serum insulin excursions following intraperitoneal injection of D-glucose ($n = 8$ per genotype); # indicates P -value < 0.05 for differences of insulin levels at 0 min compared with levels at 10 min for wild-type control animals



Dyslipidemia due to sucrose feeding in mitochondrially impaired mice

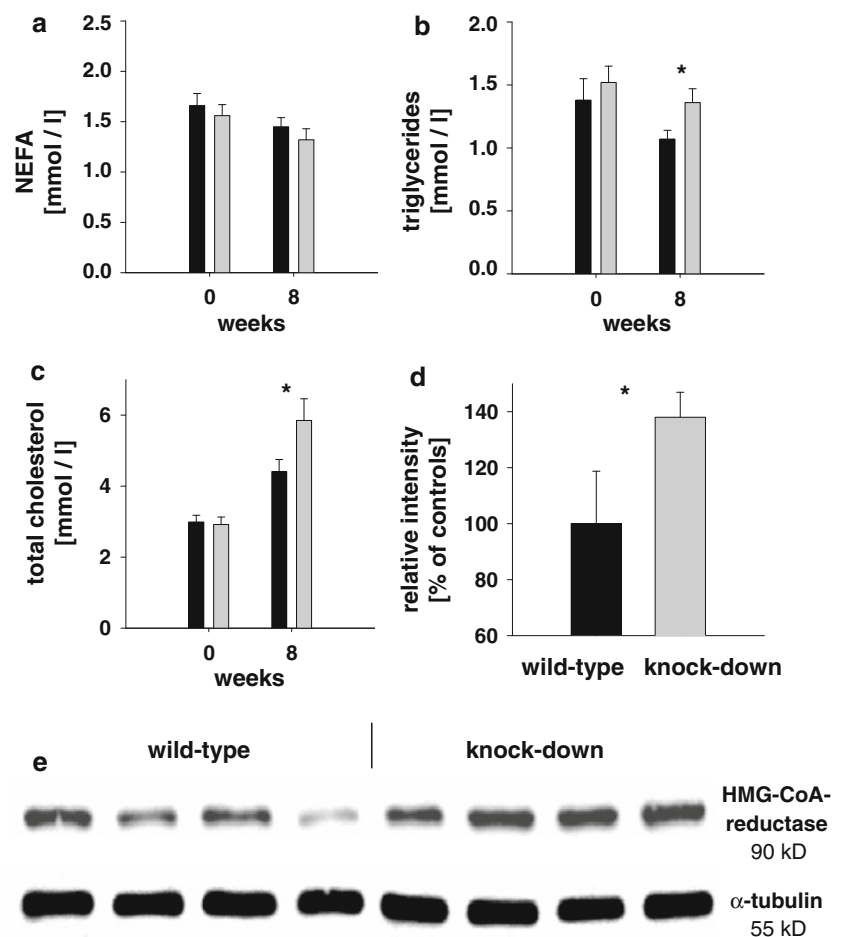
While both fasting and postprandial hyperglycemia, as well as fasting hyperinsulinemia and impaired glucose-stimulated first-phase insulin secretion are widely accepted to be indicative for type 2 diabetes mellitus and known to be independent risk factors for cardiovascular disease; we nevertheless questioned whether additional parameters contributing to the metabolic syndrome might be altered in response to impaired mitochondrial metabolism and sucrose feeding. We determined serum lipids as described before [13] in the above-mentioned state and observed no significant differences in serum concentrations for non-esterified fatty acids (NEFA) (Fig. 3a). In contrast, serum triglycerides (Fig. 3b, $P = 0.028$) and total cholesterol concentrations (Fig. 3c, $P = 0.037$) in serum from mitochondrially impaired mice on a high-sugar diet were found to be increased. Especially, since diets were depleted of

cholesterol, we hypothesized that high-sucrose feeding induces hypercholesterolemia in mitochondrially impaired mice by increasing the rate of *de novo* synthesis of this lipid. Consistent with this mechanism, we observed increased protein expression of 3-hydroxy-3-methyl-glutaryl-Coenzyme A reductase (HMG-CoA reductase, EC 1.1.1.88) (Figs. 3d [$P = 0.043$] and e), the rate-limiting step for *de novo* synthesis of cholesterol from acetyl-CoA and a key target of cholesterol-lowering drugs.

A high-fat/low-sucrose diet protects from body mass gain in mitochondrially impaired mice

While the previous set of data suggests that mitochondrial dysfunction promotes dyslipidemia and glucose intolerance following increased disaccharide uptake, we also questioned whether replacing sucrose by saturated dietary fat in an isocaloric manner would exert differential effects on metabolism. In parallel to the before-mentioned

Fig. 3 Reduced mitochondrial metabolism promotes dyslipidemia in mice on a high-sucrose diet independent of body mass. **a** Serum concentrations of non-esterified fatty acids (NEFA) in fasted animals ($n = 8$ per genotype). **b** Serum concentrations of triglycerides in fasted animals as in *Panel A* ($n = 8$ per genotype). **c** Serum concentrations of cholesterol in fasted animals as in *Panel A* ($n = 8$ per genotype). **d, e** Western blot of hepatic tissues from random-fed animals as in *Panel A* using an primary antibodies raised against HMG-CoA reductase and α -tubulin. **d** Densitometric quantification of HMG-CoA-reductase signal intensities normalized to wild-type control signals on western blots of hepatic tissues from random-fed animals ($n = 4$ per genotype); **e** native blot



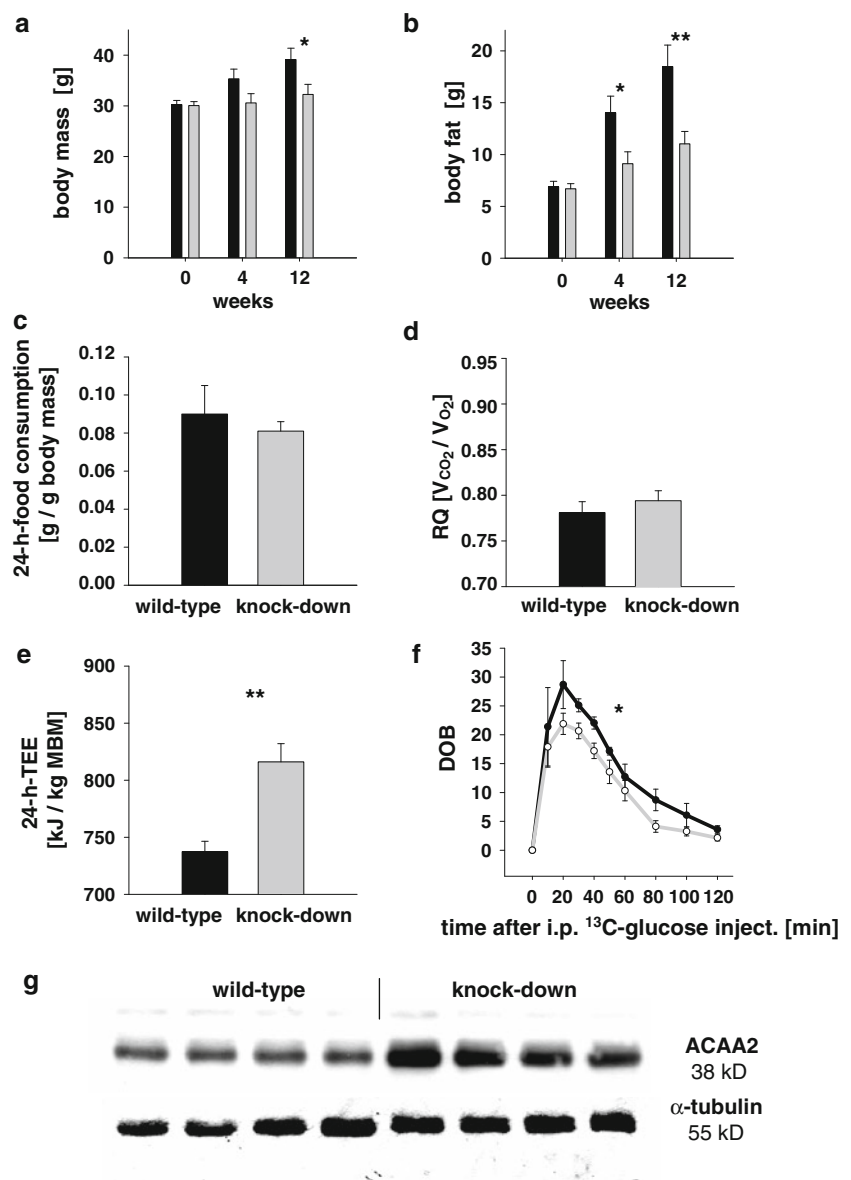
experiments, we placed both knock-down and control littermates of the above-mentioned sucrose-fed study group at the exact same age on a high-fat/low-sucrose diet (see Table 1 for details). Unexpectedly, applying this type of high-fat, Atkins-type regimen prevented body mass gain in mitochondrially impaired mice only (Fig. 4a), while control animals showed a significant increase in body mass over time (Fig. 4a, $P = 0.033$). This increase in body mass was preceded by a pronounced increase in body fat content in control mice only while mitochondrially impaired mice accumulated significantly less body fat (Fig. 4b, 4 weeks: $P = 0.021$, and 12 weeks: $P = 0.006$, respectively). Unlike for frataxin knock-down mice on a high-sucrose diet, food uptake was similar in both groups (Fig. 4c) while the respiratory quotient was similar in both groups as well (Fig. 4d) albeit lower than in the high-sucrose animals, as to be expected. However, it should be emphasized that ketones and/or glucose concentrations in urine samples were not determined; hence, ketonuria and/or glucosuria cannot be excluded to be a contributing factor affecting body mass and/or glucose metabolism.

Increased beta-oxidation paralleled by impaired substrate oxidation in high-fat fed mitochondrially impaired mice

Unaltered food uptake paralleled by differences in body fat accumulation and body mass suggest significant differences in energy conversion. To test this we first determined total energy expenditure in mitochondrially impaired mice on a high-fat diet (Fig. 4e, $P = 0.002$) and observed a striking induction of this parameter in the mitochondrially impaired animals protected from weight gain.

Next, we quantified oxidation of ^{13}C -labeled glucose in mitochondrially impaired mice fed a high-fat diet. The conversion of ^{13}C -glucose to $^{13}\text{CO}_2$ was found to be lower ($P = 0.017$ at 40 min) in frataxin knock-down genotype when compared to wild-type mice (Fig. 4f). The area under the curve (AUC) values were 1675 ± 84 delta over baseline values (DOB) and 1236 ± 90 DOB in wild-type and knock-down genotype, respectively. This effect was to be expected in frataxin knock-down mice based on reduced expression of a protein that affects Krebs cycle rate [27] by impairing activity of mitochondrial aconitase [28, 29, 32].

Fig. 4 Reduced mitochondrial metabolism protects from body mass gain by elevation of energy expenditure and beta-oxidation of fatty acids on a high-fat diet. **a** Body mass in mice ($n = 10$ per genotype); **b** body fat content in mice as in Panel A ($n = 10$ per genotype). **c** Food uptake per individual mouse, depicted for mice as in Panel A ($n = 6$ per genotype). **d** Individual respiratory quotient of mice ($n = 6$ per genotype). **e** Total energy expenditure of mice as in Panel D ($n = 6$ per genotype). **f** ^{13}C -enrichment in exhaled CO_2 expressed as DOB ($n = 5$ per genotype) after intraperitoneal injection of ^{13}C -labeled glucose. **g** Western blot of hepatic tissues from random-fed animals as in Panel A using primary antibodies raised against ACAA2 and α -tubulin



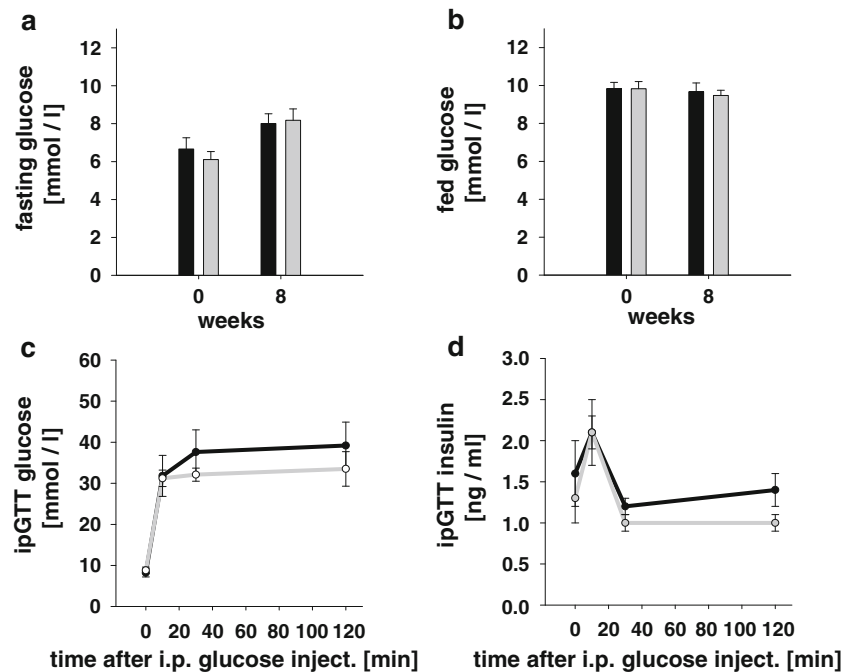
On the other hand, this reduction in glucose oxidation rate due to impaired Krebs cycle capacity cannot explain an increase in total energy expenditure in states of nutritive excess of saturated fatty acids. Therefore, we next quantified various enzymes of fatty acid metabolism, and most prominently found expression levels of acetyl-Coenzyme A acyltransferase 2 (ACAA2, also known as mitochondrial 3-oxoacyl-Coenzyme A thiolase) (EC:2.3.1.16) to be increased in mitochondrially impaired mice on a high-fat diet (Fig. 4g). Together with the before-mentioned decrease in glucose oxidation capacity (Fig. 4f), this latter finding suggests that mitochondrial dysfunction due to frataxin deficiency induces the rate-limiting step of beta-oxidation to generate C_2 intermediates, which cannot be further metabolized due to impaired Krebs cycle capacity

[27, 29, 32]. Notably, almost identical metabolic sequelae have been recently proposed for the induction of insulin resistance by saturated fatty acids [15].

Relative impairment of glucose metabolism in high-fat fed mitochondrially impaired mice

Both decreased body mass as well as reduced body fat content are known to promote glucose metabolism in mice. We therefore assumed that mice on a high-fat diet might exhibit improved glucose metabolism in comparison with control mice, since the latter are significantly more obese (Fig. 4a, b). On the other hand, if a metabolic imbalance of increased fatty acid oxidation and reduced Krebs cycle capacity promotes or even causes impaired insulin action

Fig. 5 Reduced mitochondrial metabolism does not alter glucose metabolism in mice on a high-fat diet. **a** Fasting serum glucose levels of mice that were food deprived for 16 h ($n = 8$ per genotype). **b** Postprandial serum glucose levels of mice that had free access to fat-enriched diet ($n = 8$ per genotype). **c** Serum glucose excursions following intraperitoneal injection of D-glucose; **d** Serum insulin excursions following intraperitoneal injection of D-glucose ($n = 8$ per genotype)



as previously suggested [15], the opposite might apply: Whereas the lack of increased body fat in our mitochondrially impaired mice (Fig. 4a, b) should promote glucose metabolism, this might be outweighed the metabolic imbalance within the mitochondria (Fig. 4f, g) culminating in unaltered glucose metabolism despite differences in body fat and body mass. Indeed, and despite reduced body mass and body fat content, we were unable to observe any differences in regards to serum glucose concentrations neither in the fasting (Fig. 5a) nor the postprandial, random-fed (Fig. 5b) state. Moreover, an intraperitoneal glucose challenge did not reveal any differences in glucose disappearance rates (Fig. 5c), and—unlike in sucrose-fed littermates (Fig. 2e)—insulin secretion was unaltered in both high-fat fed groups (Fig. 5d) suggesting a similar degree of insulin resistance [14] despite significant differences in body mass and body fat (Fig. 4a, b). These findings are consistent with alterations of mitochondrial lipid metabolism causing a relative impairment of glucose metabolism despite increased energy expenditure and decreased body mass at the same time, strongly supporting a recently proposed mechanism [15] where increased breakdown of fatty acids together with impaired Krebs cycle activity were shown to cause insulin resistance.

High-fat diet specifically affects expression of mitochondrial genes in mitochondrially impaired mice

To further validate our findings on increased mitochondrial lipid oxidation in mice with impaired energy metabolism

and receiving a high-fat diet, we performed microarray gene expression analysis in liver and muscle samples from mice maintained on both diets.

In animals with impaired mitochondria receiving high-fat diet feeding, we observed an unexpected positive enrichment of pathways which are associated with lipid metabolism and mitochondrial energy metabolism in both muscle and liver (supplemental Tables 1, 2). We attribute this marked increase of mitochondrial gene expression levels to a counter regulatory mechanism that is activated due to dysfunctional maturation of iron-sulfur cluster-containing enzymes in tissues with reduced expression of frataxin. In this line, we also observe increased expression of frataxin mRNA in our microarray data, which is likely due to multiple probes which hybridize to different areas of the frataxin mRNA which are not affected by cre-mediated recombination and which hints toward autoregulatory mechanisms of frataxin expression.

Increased expression of mitochondrial genes could also be due to a surplus of metabolites coming from the initial steps of beta-oxidation. In fact, among those gene sets which were up-regulated in skeletal muscle of animals with mitochondrial impairment, we also found increased expression levels of several genes which are involved in mitochondrial fatty acid import and all subsequent steps of mitochondrial beta-oxidation, such as carnitine palmitoyl-transferase and ACAA2, which is also consistent with the increased protein levels (Fig. 4g) observed in livers of high-fat fed animals with mitochondrial impairment (supplemental Table 3). In line with our previous observation, we observe a prevalence of negative enrichment, i.e.

reduced expression, of mitochondrial gene sets in liver samples from mice receiving the high-sucrose/low-fat diet (supplemental Tables 1, 2).

Choice of macronutrients determines metabolic consequences of mitochondrial dysfunction in mice

In line with the fact that physical exercise is an efficient inducer of mitochondrial metabolism known to extend life span by decreasing mortality from cardiovascular causes and/or impaired glucose metabolism [34] independently of body mass [12]; our findings indicate that impaired mitochondrial metabolism results in sucrose-induced changes to four independent risk factors for cardiovascular disease, including impaired glucose metabolism, fasting hyperinsulinemia, reduced glucose-stimulated insulin secretion, increased serum triglycerides, and elevated cholesterol levels due to increased expression of HMG-CoA reductase. Notably, these factors occur independent of increased body weight or obesity, since the sucrose-enriched diet in the current study did not cause significant differences in body mass between the different genotypes. While it is possible that sucrose promotes body weight gain in humans, our current findings suggest that additional risk factors may be induced by increased sucrose consumption, some of which are not readily detectable in epidemiological studies.

In contrast, replacing sucrose-contained calories by dietary fat, as suggested by the popular Atkins' diet regimen [4], prevents body weight gain only in states of impaired mitochondrial function when applied to our current murine model. This appears to be consistent with the fact that a high-fat, low-carbohydrate, ad libitum-available diet promotes weight loss more efficiently than conventional calorie restriction in humans [9]. Nevertheless, our findings suggest that this amelioration of body mass gain does not promote insulin sensitivity, indicating that body fat content may be of limited use in predicting overall metabolic health in states of mild mitochondrial dysfunction.

In summary, our results suggest that mitochondrial dysfunction may cause sucrose to become a multifunctional cardiovascular risk factor in mice, while high-fat/low-sugar diets may efficiently prevent weight gain without positively affecting glucose metabolism.

Acknowledgments The excellent technical assistance of Petra Albrecht, Beate Laube, Carola Plaue, Susann Richter, Waltraud Scheiding, and Elke Thom is gratefully acknowledged. The authors thank Dr. Michel Koenig for providing *frataxin* loxP mice, and Dr. Barbara B. Kahn for providing *aP2cre* mice. Grants: This study was funded by grants of the Deutsche Forschungsgemeinschaft (RI 1076/1-3) and the Wilhelm-Sander-Stiftung (both to M.R.).

Conflict of interest statement None.

References

1. Abel ED, Peroni O, Kim JK, Kim YB, Boss O, Hadro E, Minnemann T, Shulman GI, Kahn BB (2001) Adipose-selective targeting of the GLUT4 gene impairs insulin action in muscle and liver. *Nature* 409:729–733
2. Astrup A, Buemann B, Toubro S, Raben A (1996) Defects in substrate oxidation involved in the predisposition to obesity. *Proc Nutr Soc* 55:817–828
3. Astrup A, Meinert Larsen T, Harper A (2004) Atkins and other low-carbohydrate diets: hoax or an effective tool for weight loss? *Lancet* 364:897–899
4. Atkins RC (1973) *Dr. Atkins' Diet Revolution*. Bantam, New York
5. Berglund L, Lefevre M, Ginsberg HN, Kris-Etherton PM, Elmer PJ, Stewart PW, Ershow A, Pearson TA, Dennis BH, Roheim PS, Ramakrishnan R, Reed R, Stewart K, Phillips KM (2007) Comparison of monounsaturated fat with carbohydrates as a replacement for saturated fat in subjects with a high metabolic risk profile: studies in the fasting and postprandial states. *Am J Clin Nutr* 86:1611–1620
6. Bravata DM, Sanders L, Huang J, Krumholz HM, Olkin I, Gardner CD (2003) Efficacy and safety of low-carbohydrate diets: a systematic review. *JAMA* 289:1837–1850
7. Di Piero D, Tavazzi B, Perno CF, Bartolini M, Balestra E, Calio R, Giardina B, Lazzarino G (1995) An ion-pairing high-performance liquid chromatographic method for the direct simultaneous determination of nucleotides, deoxynucleotides, nicotinic coenzymes, oxypurines, nucleosides, and bases in perchloric acid cell extracts. *Anal Biochem* 231:407–412
8. Drewnowski A (2003) Fat and sugar: an economic analysis. *J Nutr* 133:838S–840S
9. Foster GD, Wyatt HR, Hill JO, McGuckin BG, Brill C, Mohammed BS, Szapary PO, Rader DJ, Edman JS, Klein S (2003) A randomized trial of a low-carbohydrate diet for obesity. *N Engl J Med* 348:2082–2090
10. Friedman MI (1998) Fuel partitioning and food intake. *Am J Clin Nutr* 67:513S–518S
11. Howard BV, Wylie-Rosett J (2002) Sugar and cardiovascular disease: a statement for healthcare professionals from the Committee on Nutrition of the Council on Nutrition, Physical Activity, and Metabolism of the American Heart Association. *Circulation* 106:523–527
12. Hu FB, Willett WC, Li T, Stampfer MJ, Colditz GA, Manson JE (2004) Adiposity as compared with physical activity in predicting mortality among women. *N Engl J Med* 351:2694–2703
13. Jürgens H, Haass W, Castaneda TR, Schürmann A, Koebnick C, Dombrowski F, Otto B, Nawrocki AR, Scherer PE, Spranger J, Ristow M, Joost HG, Havel PJ, Tschöp MH (2005) Consuming fructose-sweetened beverages increases body adiposity in mice. *Obes Res* 13:1146–1156
14. Kahn CR (1994) Banting Lecture: insulin action, diabetogenesis, and the cause of type II diabetes. *Diabetes* 43:1066–1084
15. Koves TR, Ussher JR, Noland RC, Slentz D, Mosedale M, Ilkayeva O, Bain J, Stevens R, Dyck JR, Newgard CB, Lopaschuk GD, Muoio DM (2008) Mitochondrial overload and incomplete fatty acid oxidation contribute to skeletal muscle insulin resistance. *Cell Metab* 7:45–56
16. Lichtenstein AH, Appel LJ, Brands M, Carnethon M, Daniels S, Franch HA, Franklin B, Kris-Etherton P, Harris WS, Howard B, Karanja N, Lefevre M, Rudel L, Sacks F, Van Horn L, Winston M, Wylie-Rosett J (2006) Diet and lifestyle recommendations revision 2006: a scientific statement from the American Heart Association Nutrition Committee. *Circulation* 114:82–96

17. Mann JI (2002) Diet and risk of coronary heart disease and type 2 diabetes. *Lancet* 360:783–789
18. McGarry JD (1998) Glucose-fatty acid interactions in health and disease. *Am J Clin Nutr* 67:500S–504S
19. Mootha VK, Lindgren CM, Eriksson KF, Subramanian A, Sihag S, Lehar J, Puigserver P, Carlsson E, Ridderstrale M, Laurila E, Houstis N, Daly MJ, Patterson N, Mesirov JP, Golub TR, Tamayo P, Spiegelman B, Lander ES, Hirschhorn JN, Altshuler D, Groop LC (2003) PGC-1 α -responsive genes involved in oxidative phosphorylation are coordinately downregulated in human diabetes. *Nat Genet* 34:267–273
20. Nordmann AJ, Nordmann A, Briel M, Keller U, Yancy WS Jr, Brehm BJ, Bucher HC (2006) Effects of low-carbohydrate vs low-fat diets on weight loss and cardiovascular risk factors: a meta-analysis of randomized controlled trials. *Arch Intern Med* 166:285–293
21. Petzke KJ, Feist T, Fleig WE, Metges CC (2006) Nitrogen isotopic composition in hair protein is different in liver cirrhotic patients. *Rapid Commun Mass Spectrom* 20:2973–2978
22. Pomplun D, Voigt A, Schulz TJ, Thierbach R, Pfeiffer AFH, Ristow M (2007) Reduced expression of mitochondrial frataxin in mice exacerbates diet-induced obesity. *Proc Natl Acad Sci* 104:6377–6381
23. Popkin BM, Nielsen SJ (2003) The sweetening of the world's diet. *Obes Res* 11:1325–1332
24. Puccio H, Simon D, Cossee M, Criqui-Filipe P, Tiziano F, Melki J, Hindelang C, Matyas R, Rustin P, Koenig M (2001) Mouse models for Friedreich ataxia exhibit cardiomyopathy, sensory nerve defect and Fe-S enzyme deficiency followed by intramitochondrial iron deposits. *Nat Genet* 27:181–186
25. Reaven GM (2005) Why syndrome X? from Harold Himsworth to the insulin resistance syndrome. *Cell Metab* 1:9–14
26. Ristow M, Mulder H, Pomplun D, Schulz TJ, Müller-Schmehl K, Krause A, Fex M, Puccio H, Müller J, Isken F, Spranger J, Müller-Wieland D, Magnuson MA, Möhlig M, Koenig M, Pfeiffer AFH (2003) Frataxin-deficiency in pancreatic islets causes diabetes due to loss of beta-cell mass. *J Clin Invest* 112:527–534
27. Ristow M, Pfister MF, Yee AJ, Schubert M, Michael L, Zhang CY, Ueki K, Michael MD 2nd, Lowell BB, Kahn CR (2000) Frataxin activates mitochondrial energy conversion and oxidative phosphorylation. *Proc Natl Acad Sci U S A* 97:12239–12243
28. Rötig A, de Lonlay P, Chretien D, Foury F, Koenig M, Sidi D, Munnich A, Rustin P (1997) Aconitase and mitochondrial iron-sulphur protein deficiency in Friedreich ataxia. *Nat Genet* 17:215–217
29. Schulz TJ, Thierbach R, Voigt A, Drewes G, Mietzner BH, Steinberg P, Pfeiffer AF, Ristow M (2006) Induction of oxidative metabolism by mitochondrial frataxin inhibits cancer growth: Otto Warburg revisited. *J Biol Chem* 281:977–981
30. Subramanian A, Tamayo P, Mootha VK, Mukherjee S, Ebert BL, Gillette MA, Paulovich A, Pomeroy SL, Golub TR, Lander ES, Mesirov JP (2005) Gene set enrichment analysis: a knowledge-based approach for interpreting genome-wide expression profiles. *Proc Natl Acad Sci U S A* 102:15545–15550
31. Taubes G (2001) The soft science of dietary fat. *Science* 291:2536–2545
32. Thierbach R, Schulz TJ, Isken F, Voigt A, Mietzner B, Drewes G, von Kleist-Retzow JC, Wiesner RJ, Magnuson MA, Puccio H, Pfeiffer AF, Steinberg P, Ristow M (2005) Targeted disruption of hepatic frataxin expression causes impaired mitochondrial function, decreased life span, and tumor growth in mice. *Hum Mol Genet* 14:3857–3864
33. Volek JS, Sharman MJ, Forsythe CE (2005) Modification of lipoproteins by very low-carbohydrate diets. *J Nutr* 135:1339–1342
34. Warburton DE, Nicol CW, Bredin SS (2006) Health benefits of physical activity: the evidence. *Can Med Ass J (CMAJ)* 174:801–809
35. Yanovski SZ, Yanovski JA (2002) Obesity. *N Engl J Med* 346:591–602
36. Yudkin J (1978) Dietary factors in arteriosclerosis: sucrose. *Lipids* 13:370–372

Supplementary Legends:

Supplementary Table 1: Scores for the top 20 pathways with enrichment of up-regulated (positive enrichment, blue background) or down-regulated (negative enrichment, red background) gene expression patterns. Groups appear in the order: muscle, high fat diet; liver, high fat diet; muscle, high-sucrose diet; liver, high-sucrose diet.

Supplementary Table 2: Summary of mitochondrial genes expressed at a fold change of >1.5 in knock-down animals compared to control animals. Dietary regimen and tissue as indicated.

Supplementary Table 3: Summary of genes involved in mitochondrial lipid import and oxidation in skeletal muscle from animals feeding on high fat diet.

	HFD_muscle_control vs knock-down		HFD_liver_control vs knock-down	
pathway score	Top 20 positive enrichment pathways	Top20 negative enrichment pathways	Top 20 positive enrichment pathways	Top20 negative enrichment pathways
1	SKELETAL_DEVELOPMENT	IMMUNE_RESPONSE	LIPID_METABOLIC_PROCESS	IMMUNE_RESPONSE
2	OXIDOREDUCTASE_ACTIVITY	IMMUNE_SYSTEM_PROCESS	CELLULAR_LIPID_METABOLIC_PROCESS	IMMUNE_SYSTEM_PROCESS
3	MITOCHONDRION	CELL_ACTIVATION	MEMBRANE_FRACTION	CELL_DEVELOPMENT
4	MITOCHONDRIAL_PART	HEMOPOIETIC_OR_LYMPHOID_ORGAN_DEVELOPMENT	HYDROLASE_ACTIVITY__ACTING_ON_ESTERS	SYSTEM_PROCESS
5	LIPID_BINDING	IMMUNE_SYSTEM_DEVELOPMENT	NERVOUS_SYSTEM_DEVELOPMENT	PROGRAMMED_CELL_DEATH
6	GENERATION_OF_PRECURSOR_METABOLITE	CHEMOKINE_ACTIVITY	GOLGI_APPARATUS	CYTOSKELETON
7	CARBOXYLIC_ACID_METABOLIC_PROCESS	CELLULAR_DEFENSE_RESPONSE	G_PROTEIN_COUPLED_RECEPTOR_PROTEIN_SIGNALING	POSITIVE_REGULATION_OF_BIOLOGICAL_PROCESS
8	LIPID_METABOLIC_PROCESS	CHEMOKINE_RECEPTOR_BINDING	MITOCHONDRION	NON_MEMBRANE_BOUND_ORGANELLE
9	PROTEINACEOUS_EXTRACELLULAR_MATRIX	CYTOKINE_BINDING	RNA_BINDING	POSITIVE_REGULATION_OF_CATALYTIC_ACTIVITY
10	OXIDOREDUCTASE_ACTIVITY_GO_0016611	LOCOMOTORY_BEHAVIOR	(no other enriched pathways)	DEFENSE_RESPONSE
11	MITOCHONDRIAL_ENVELOPE	JAK_STAT_CASCADE		POSITIVE_REGULATION_OF_CELLULAR_PROCESS
12	MITOCHONDRIAL_INNER_MEMBRANE	CELL_CYCLE_PHASE		CYTOSKELETAL_PART
13	MONOCARBOXYLIC_ACID_METABOLIC_PROCESS	CELL_CYCLE_PROCESS		RECEPTOR_BINDING
14	EXTRACELLULAR_REGION	CYTOKINE_ACTIVITY		ORGAN_DEVELOPMENT
15	EXTRACELLULAR_REGION_PART	POSITIVE_REGULATION_OF_CELLULAR_PROTEIN_METABOLIC_PROCESS		ACTIN_FILAMENT_BASED_PROCESS
16	NADH_DEHYDROGENASE_COMPLEX	PROTEIN_DOMAIN_SPECIFIC_BINDING		HOMEOSTATIC_PROCESS
17	MITOCHONDRIAL_MEMBRANE	PHOSPHOPROTEIN_PHOSPHATASE_ACTIVITY		REGULATION_OF_MOLECULAR_FUNCTION
18	MITOCHONDRIAL_RESPIRATORY_CHAIN_COMPLEX	BEHAVIOR		REGULATION_OF_PROGRAMMED_CELL_DEATH
19	EXTRACELLULAR_MATRIX	MITOSIS		REGULATION_OF_APOPTOSIS
20	ION_TRANSPORT	POSITIVE_REGULATION_OF_PROTEIN_METABOLIC_PROCESS		CYTOSKELETON_ORGANIZATION_AND_BIOGENESIS

Carbohydrate diet_muscle_control vs knock-down		Carbohydrate diet_liver_control vs knock-down	
Top 20 positive enrichment pathways	Top20 negative enrichment pathways	Top 20 positive enrichment pathways	Top20 negative enrichment pathways
REGULATION_OF_CELL_ADHESION GROWTH STEROID_METABOLIC_PROCESS EXTRACELLULAR_MATRIX EXOPEPTIDASE_ACTIVITY ALCOHOL_METABOLIC_PROCESS SERINE_HYDROLASE_ACTIVITY CALCIUM_ION_BINDING EXTRACELLULAR_SPACE PROTEIN_CATABOLIC_PROCESS BIOPOLYMER_CATABOLIC_PROCESS PROTEOLYSIS MACROMOLECULE_CATABOLIC_PROCESS EXTRACELLULAR_REGION_PART CATABOLIC_PROCESS PEPTIDASE_ACTIVITY ENDOPEPTIDASE_ACTIVITY EXTRACELLULAR_REGION CELLULAR_LIPID_METABOLIC_PROCESS LIPID_METABOLIC_PROCESS	DEFENSE_RESPONSE IMMUNE_SYSTEM_PROCESS RESPONSE_TO_WOUNDING ION_HOMEOSTASIS M_PHASE_OF_MITOTIC_CELL_CYCLE INFLAMMATORY_RESPONSE RESPONSE_TO_EXTERNAL_STIMULUS MITOSIS SPINDLE IMMUNE_RESPONSE CELLULAR_HOMEOSTASIS CHROMOSOMAL_PART RESPONSE_TO_OTHER_ORGANISM CHROMOSOME MITOTIC_CELL_CYCLE CHROMOSOME_SEGREGATION CELL_CYCLE_PROCESS M_PHASE CHROMATIN_BINDING CHEMICAL_HOMEOSTASIS	RESPONSE_TO_EXTERNAL_STIMULUS LOCOMOTORY_BEHAVIOR DEFENSE_RESPONSE BEHAVIOR RESPONSE_TO_WOUNDING CALCIUM_ION_BINDING IMMUNE_RESPONSE INFLAMMATORY_RESPONSE RESPONSE_TO_CHEMICAL_STIMULUS CATION_BINDING IMMUNE_SYSTEM_PROCESS ION_BINDING CATION_HOMEOSTASIS REGULATION_OF_BIOLOGICAL_QUALITY CHEMICAL_HOMEOSTASIS CELLULAR_CATION_HOMEOSTASIS CELLULAR_HOMEOSTASIS ION_HOMEOSTASIS G_PROTEIN_COUPLED_RECEPTOR_BINDING HOMEOSTATIC_PROCESS	ORGANIC_ACID_METABOLIC_PROCESS MITOCHONDRION CARBOXYLIC_ACID_METABOLIC_PROCESS CATION_TRANSMEMBRANE_TRANSPORTER_ACTIVIT ION_TRANSMEMBRANE_TRANSPORTER_ACTIVITY REGULATION_OF_RNA_METABOLIC_PROCESS REGULATION_OF_TRANSCRIPTION_DNA_DEPENDEI ENZYME_LINKED_RECEPTOR_PROTEIN_SIGNALING ORGANELLE_ENVELOPE ENVELOPE NUCLEOPLASM MEMBRANE_ENCLOSED_LUMEN ORGANELLE_LUMEN RNA_METABOLIC_PROCESS NEUROLOGICAL_SYSTEM_PROCESS TRANSCRIPTION_COACTIVATOR_ACTIVITY SUBSTRATE_SPECIFIC_TRANSMEMBRANE_TRANSPC LIPID_METABOLIC_PROCESS TRANSCRIPTION_DNA_DEPENDENT RNA_BIOSYNTHETIC_PROCESS

Gene Set Enrichment Analysis (GSEA)			
Positive enrichment			
High fat diet_liver_control vs knock-down			
Affymetrix ID	Gene Symbol	Gene Title	Regulation (fold change)
1419339_at	NEU3	neuraminidase 3	2,932551384
1449685_s_at	OXSM	3-oxoacyl-ACP synthase, mitochondrial	2,732240438
1417709_at	CYP46A1	cytochrome P450, family 46, subfamily a, polypeptide 1	2,551020384
1434204_x_at	SHMT2	Serine hydroxymethyl transferase 2 (mitochondrial)	2,352941275
1448300_at	MGST3	microsomal glutathione S-transferase 3	2,298850536
1418075_at	ST6GALNAC4	ST6 (alpha-N-acetyl-neuraminyl-2,3-beta-galactosyl-1,3)-N-acetylglucosaminyl transferase 4	2,183406115
1422076_at	ACOT4	acyl-CoA thioesterase 4	2,137449503
1428160_at	NDUFAB1	NADH dehydrogenase (ubiquinone) 1, alpha/beta subcomplex, 1	1,972386599
1456577_x_at	PITRM1	pitrilysin metallopeptidase 1	1,923076868
1424190_at	PIGC	phosphatidylinositol glycan, class C	1,890359163
1420715_a_at	PPARG	peroxisome proliferator activated receptor gamma	1,862197399
1434420_x_at	TOMM22	translocase of outer mitochondrial membrane 22 homolog (yeast)	1,845018506
1422700_at	ALOX12	arachidonate 12-lipoxygenase	1,831501842
1417273_at	PDK4	pyruvate dehydrogenase kinase, isoenzyme 4	1,805054188
1421268_at	UGCG	UDP-glucose ceramide glucosyltransferase	1,801801801
1418655_at	B4GALNT1	beta-1,4-N-acetyl-galactosaminyl transferase 1	1,769911528
1425994_a_at	ASAH2	N-acylsphingosine amidohydrolase 2	1,721170425
1424868_at	GLYAT	glycine-N-acyltransferase	1,71526587
1420541_at	RDH16	retinol dehydrogenase 16	1,712328792
1450383_at	LDLR	low density lipoprotein receptor	1,709401727
1436756_x_at	HADH	hydroxyacyl-Coenzyme A dehydrogenase	1,661129594
1449065_at	ACOT1	acyl-CoA thioesterase 1	1,631321311
1450776_at	AGPAT6	1-acylglycerol-3-phosphate O-acyltransferase 6 (lysophosphatidic acid acyltransferase)	1,612903237
1435275_at	COX6B2	cytochrome c oxidase subunit VIb polypeptide 2	1,612903237
1434099_at	PPARGC1A	Peroxisome proliferative activated receptor, gamma, coactivator 1 alpha	1,608867109
1449078_at	ST3GAL6	ST3 beta-galactoside alpha-2,3-sialyltransferase 6	1,57977879
1416839_at	MUT	methylmalonyl-Coenzyme A mutase	1,555209994
1437680_x_at	GLRX2	glutaredoxin 2 (thioltransferase)	1,52207005
1415776_at	ALDH3A2	aldehyde dehydrogenase family 3, subfamily A2	1,50150156
1435352_at	PIGK	phosphatidylinositol glycan, class K	1,50150156
1425519_a_at	CD74	CD74 antigen (invariant polypeptide of major histocompatibility complex class II)	-3,026000023
1415904_at	LPL	lipoprotein lipase	-2,650000095
1418203_at	PMAIP1	phorbol-12-myristate-13-acetate-induced protein 1	-2,434999943
1426538_a_at	TP53	tumor protein p53 (Li-Fraumeni syndrome)	-2,358000004
1433952_at	TUFM	Tu translation elongation factor, mitochondrial	-2,250999928
1416022_at	FABP5	fatty acid binding protein 5, epidermal	-1,906999946
1427698_at	BRCA1	breast cancer 1	-1,825000048
1438809_at	ATP5C1	ATP synthase, H+ transporting, mitochondrial F1 complex, gamma subunit	-1,787999988
1424562_a_at	SLC25A4	solute carrier family 25 (mitochondrial carrier, adenine nucleotide transporter)	-1,720500052
1455804_x_at	OXCT1	3-oxoacid CoA transferase 1	-1,695000052
1417696_at	SOAT1	sterol O-acyltransferase 1	-1,595000029
1419270_a_at	DUT	deoxyuridine triphosphatase	-1,582000017
1422468_at	PPT1	palmitoyl-protein thioesterase 1	-1,572000027
1436448_a_at	PTGS1	prostaglandin-endoperoxide synthase 1	-1,547999978
1423738_at	OXA1L	oxidase assembly 1-like	-1,531999946

High fat diet_muscle_control vs knock-down			
Affymetrix ID	Gene Symbol	Gene Title	Regulation (fold change)
1449065_at	ACOT1	acyl-CoA thioesterase 1	2,824858665
1435630_s_at	ACAT2	acetyl-Coenzyme A acetyltransferase 2	2,267573595
1452341_at	ECHS1	enoyl Coenzyme A hydratase, short chain, 1, mitochondrial	1,972386599
1437172_x_at	HADHB	hydroxyacyl-Coenzyme A dehydrogenase/3-ketoacyl-Coenzyme	1,949317694
1424184_at	ACADVL	acyl-Coenzyme A dehydrogenase, very long chain	1,90114069
1455972_x_at	HADH	hydroxyacyl-Coenzyme A dehydrogenase	1,852332711
1451271_a_at	ACAT1	acetyl-Coenzyme A acetyltransferase 1	1,837401628
1418328_at	CPT1B	carnitine palmitoyltransferase 1b, muscle	1,821493626
1419262_at	ACAD8	acyl-Coenzyme A dehydrogenase family, member 8	1,760563374
1416408_at	ACOX1	acyl-Coenzyme A oxidase 1, palmitoyl	1,757781148
1460216_at	ACADS	acyl-Coenzyme A dehydrogenase, short chain	1,736111164
1417008_at	CRAT	carnitine acetyltransferase	1,689189196
1415984_at	ACADM	acyl-Coenzyme A dehydrogenase, medium chain	1,636661172
1448987_at	ACADL	acyl-Coenzyme A dehydrogenase, long-chain	1,62074554
1448382_at	EHHADH	enoyl-Coenzyme A, hydratase/3-hydroxyacyl Coenzyme A dehyd	1,618122935
1438156_x_at	CPT1A	carnitine palmitoyltransferase 1a, liver	1,615508914
1449457_at	ACOT12	acyl-CoA thioesterase 12	1,605136395
1455446_x_at	ACADSB	acyl-Coenzyme A dehydrogenase, short/branched chain	1,529052019